Available online at www.sciencedirect.com

jmr&t Journal of Materials Research and Technology

journal homepage: www.elsevier.com/locate/jmrt

Original Article

Improvement of corrosion properties of plasma in an aluminum alloy 6061-T6 by phytic acid anodization temperature

Minjoong Kim [a,b,1], *Eunmi Choi* [b,1], *Jongho So* [a,b], *Jae-Soo Shin* [c], *Chin-Wook Chung* [a], *Seon-Jeong Maeng* [b], *Ju-Young Yun* [b,d,*]

[a] *Department of Electrical Engineering, Hanyang University, Seoul, 04763, Republic of Korea*
[b] *Vacuum Materials Measurement Team, Korea Research Institute of Standards and Science (KRISS), Daejeon, 34113, Republic of Korea*
[c] *Department of Advanced Materials Engineering, Daejeon University, Daejeon, 34520, Republic of Korea*
[d] *Department of Nanomaterials Science and Engineering, University of Science and Technology, Daejeon, 34113, Republic of Korea*

ARTICLE INFO

Article history:
Received 14 May 2020
Accepted 22 December 2020
Available online 31 December 2020

Keywords:
Phytic acid
Anodization
Aluminum oxide
Corrosion properties
Plasma resistance

ABSTRACT

We report on the formation of anodic aluminum oxide (AAO) film using phytic acid ($C_6H_{18}O_{24}P_6$), a naturally obtainable and non-toxic organic acid electrolyte. When the temperature of the phytic acid electrolytes changes from 0 °C to 20 °C, the pore size increases, and the AAO film becomes less dense because the growth rate of the AAO film increases. In particular, when the temperature of the phytic acid electrolyte is above 15 °C, the AAO film changes dramatically. According to XRD analysis, the alpha-alumina intensity was relatively higher in the AAO film grown at low-temperatures (0, 5, 10 °C) than high-temperatures (15, 20 °C). It was possible to obtain a result that the properties were better. The microstructural change of the AAO film according to the temperature of the phytic acid electrolytes affected the breakdown voltage and the number of contamination particles that are generated, which are important properties for plasma corrosion protection coating materials. The AAO film grown in the low-temperature has the most suitable properties for use as a plasma corrosion protection coating material. Notably, the breakdown voltage of the AAO film is 0.45 kV at 14.9 μm thickness, with no observable crack on its surface after the plasma corrosion test. These findings provide significant evidence to support the application of phytic acid as an electrolyte to grow AAOfilms, and the AAOfilm grown in a phytic acid bath can be applied as a plasma corrosion protection coating material.

* Corresponding author.
E-mail address: jyun@kriss.re.kr (J.-Y. Yun).
[1] These authors contributed equally to this work.
https://doi.org/10.1016/j.jmrt.2020.12.086

1. Introduction

Due to their high resistance against corrosion and porous structural features, anodic oxide films of aluminum alloys have been utilized in various engineering and nanoscience applications, including in membranes, nanostructures for sensors, and traditional corrosion protection, coloring, and hardening [1–6].

Anodic aluminum oxide (AAO) films have been increasingly used as commercial coatings to protect equipment from plasma corrosion during semiconductor and display manufacturing [7] because the AAO film offers corrosion resistance to the etching gases and plasma and can be implemented with a low process cost [8]. The AAO film properties, including its nanostructure, optical, chemical, physical, and mechanical properties, can change depending closely on the electrolyte species that are employed in the AAO process, and most studies related to AAO films have focused on the electrolyte [6]. Sulfuric acid and chromic acid have been commonly used as the best acid electrolytes for the anodizing process because it is possible to obtain an AAO film with sufficient thickness, high corrosion resistance, excellent adhesion to base materials, and suitable mechanical properties [1,9]. However, sulfuric acid and chromic acid are highly toxic environmental pollutants, so the use of non-toxic organic acid electrolytes, such as oxalic acid [10], tartaric acid [11], citric acid [12], adipic acid [13], and etidronic acid [14], is being considered [1,15].

Recent studies on AAO films investigated the photoluminescence, corrosion resistance, optical and mechanical properties according to the use of mixed acid electrolytes or single-acid electrolytes, such as selenic acid [16], phosphoric acid [17], malonic acid [18], and acetylene dicarboxylic acid [19]. However, there is a paucity of studies on plasma corrosion, which has recently become an important issue for the AAO film applications.

Recently, Song et al. conducted a plasma resistance of nonporous AAO film. According to them, it has been reported that as the sealing time passes, surface cracks increase, the plasma corrosion resistance decreases, and consequently, the number of contaminants generated increases [20].

Among the various acid electrolyte candidates, phytic acid is a naturally occurring, non-toxic, organic acid that contains hydroxyl groups, oxygen atoms, and phosphate carboxyl groups. Phosphoric acid and the hydroxyl groups of phytic acid are deposited on metal surfaces through reactions with metal ions that form chelate complex compounds to improve corrosion resistance and provide improved adhesion with the base material [21–24].

Shi et al. conducted the reaction mechanism of phytic acid as acid electrolytes on 2024-T3 aluminum alloy and reported on the change in the AAO films according to the pH [23]. However, the applicability of the results of the study is limited because the corrosion resistance evaluation was only performed for NaCl corrosive media. Most studies on phytic acid electrolytes employed magnesium alloy as a reaction material [21,22,25–29], and there have been few reports employing aluminum alloys as reaction materials in the plasma corrosion evaluation of AAO films.

This study improves the plasma corrosion resistance of 6061 aluminum alloy and investigates the reaction mechanism for changes in AAO film properties according to the temperature of the phytic acid bath including phytic acid electrolytes. The evaluations were carried out using field emission scanning electron microscopy (FE-SEM) and energy-dispersive X-ray spectroscopy (EDS). In addition, the applicability of the phytic acid electrolytes is discussed by evaluating the breakdown voltage and plasma corrosion resistance, an important characteristic in the use of the material as a coating for plasma corrosion protection of equipment parts in a process chamber for semiconductor and display manufacturing.

2. Experimental

2.1. Sample preparation

Polished aluminum alloy 6061-T6 (HIGGSLAB, Daejeon, Korea) in circular disks of 76.2 mm in diameter with a thickness of 3 mm were used as the substrate. Table 1 shows the chemical composition (wt. %) of aluminum alloy 6061-T6.

The substrate was cleaned by sonication for 20 min in ethanol solution (99.8%, DUKSAN Reagents, Ansan, Korea) and was dried in an N_2 gas flow. 9.5 M phytic acid solutions were prepared by dissolving phytic acid (purity > 50%, Sigma–Aldrich, St. Louis, Missouri, USA) with deionized water. Next, the substrate was anodized in a 9.5 M phytic acid solution for 180 min, and during that time, 80 V potential was constantly applied with a DC power supply (GP-2480, LNC, Incheon, Korea) (Fig. 1a). End of anodization, the AAO samples were washed with deionized water for 20 min and dried in an N_2 gas flow at room temperature. After that, the dried samples were kept in a vacuum desiccator.

2.2. Evaluation system

For the thickness of the AAO film, a thickness meter using an eddy current induction method was used (FMP 10, Helmut Fischer, Sindelfingen, Germany).

The morphologies and the elements of the film surfaces were observed via FE-SEM and EDS (S-4800, HITACHI, Tokyo, Japan). In addition, the ImageJ program (ver.1.53e, 64-bit) was used to analyze the pore area and porosity of the AAO film surface.

The structurally characterized of the AAO films was determined by X-ray diffraction analyzer (XRD, SmartLab,

Table 1 – Chemical composition of aluminum alloy 6061-T6 (wt. %).

Mg	Si	Fe	Cu	Cr	Zn	Ti	Mn	Al
0.873	0.698	0.450	0.342	0.199	0.193	0.079	0.054	Bal.

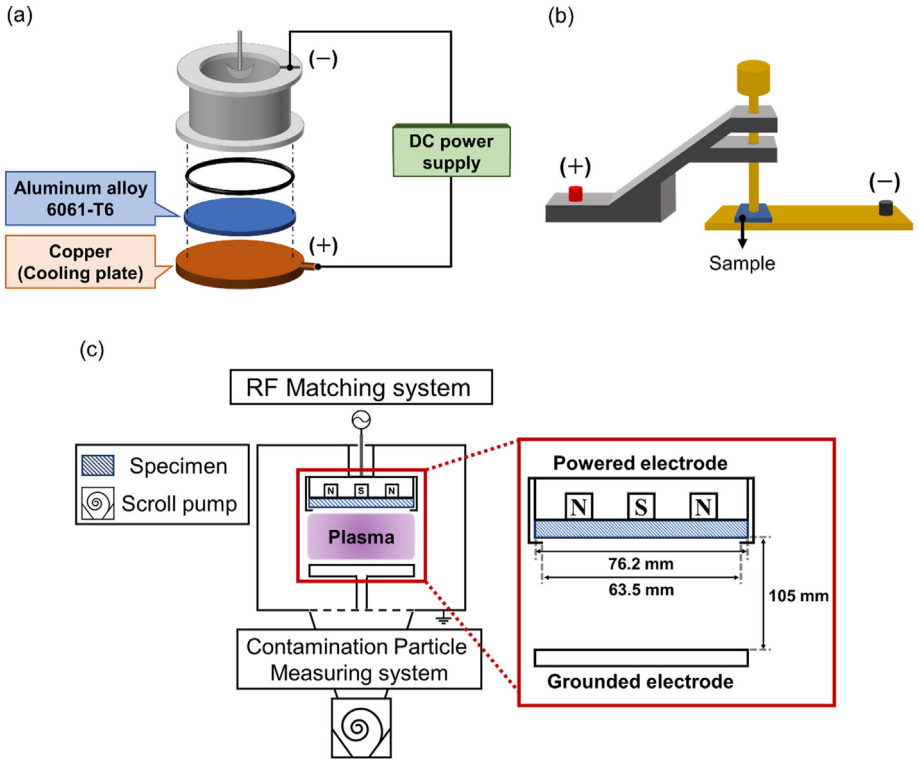

Fig. 1 – Schematic of (a) the anodizing system, (b) breakdown voltage tester, and (c) the plasma corrosion test system (CCP-RIE).

Rigaku Corporation, Japan) over the range of 10°–90° (2 θ angle) using CuKα radiation (λ = 1.54056 Å).

The electrical breakdown of the AAO film was measured using a handmade dielectric breakdown voltage measuring tool (one-electrode method) (Fig. 1b). The voltage signal was generated by a breakdown voltage tester (TOS 9201, KIKUSUI, Yokohama, Japan), and the measuring parameters and data were controlled and recorded using a handmade program (LabVIEW, Austin, Texas, USA) [30].

The plasma corrosion test was performed using a CCP-RIE (Capacitively Coupled Plasma-Reactive Ion Etching) system with etching gas (CF_4 (99.999%)/O_2 (99.995%)/Ar (99.999%)) for 60 min. The plasma maintained between two circular 76.2 mm diameter electrodes separated by a 105 mm gap and the area where the actual AAO film is exposed to plasma is circular 63.5 mm diameter (Table 2 and Fig. 1c).

3. Result and discussions

As mentioned earlier, phytic acid ($C_6H_{18}O_{24}P_6$) is a strong acid consisting of 12 hydroxyl groups, 24 oxygen atoms, and 6 phosphate groups, and it forms a strong chelate with metal ions (Fig. 2a) [13]. According to Crea et al., when phytic acid forms strong chelates with metal ions, chemical structures of 1-axial/5-equatorial or 5-axial/1-equatorial is mainly formed, and the pH of the electrolyte determines the main chelate structure [29]. Phytic acid and Al^{3+} complex have a 1:1 stoichiometry [31], and when the pH is lower than 9 in alkali metal ion solutions, the formation of 1-axial/5-equatorial chemical structures with less steric hindrance is predominant [29].

Shi et al. reported that the formable chemical structure of the composite by the Al^{3+} chelate is also predominantly the 1-axial/5-equatorial equatorial structure with low volumetric disturbances in the vertical direction [23]. As a result, the mechanism of the AAO film formation by phytic acid electrolyte is as follows [13]:

$$C_6H_{18}O_{24}P_6 \rightleftharpoons XH^+ + C_6H_{(18-X)}O_{24}P_6^{-X} (i = 12, 11, \cdots, 2, 1) \quad (1)$$

$$2Al + 6H^+ \rightarrow 2Al^{3+} + 3H_2 \quad (2)$$

$$Al^{3+} + C_6H_{(18-X)}O_{24}P_6^{-X} \rightarrow Al\left(C_6H_{(18-X)}O_{24}P_6^{-X+1}\right)_3 \quad (3)$$

Fig. 2b shows the change in the phytic acid bath pH and current density according to the electrolyte temperature. In general, it is widely known that the change in current density during the potentiostatic anodizing process takes an almost steady value after being changed from a four-step anodizing process. The current density sharply increases when starting the anodizing process and then the current density decreases slightly and has its lowest value, as the barrier layer of AAO

Table 2 – Plasma corrosion test condition using CCP-RIE system.

Plasma corrosion test condition		
Power (W)	100	
Treatment time (min)	60	
Gas (sccm)	30: 25: 5	< CF_4: O_2: Ar>
Base Pressure (mTorr)	20 ± 1	< Plasma off >
Working Pressure (mTorr)	300 ± 5	< Plasma on >

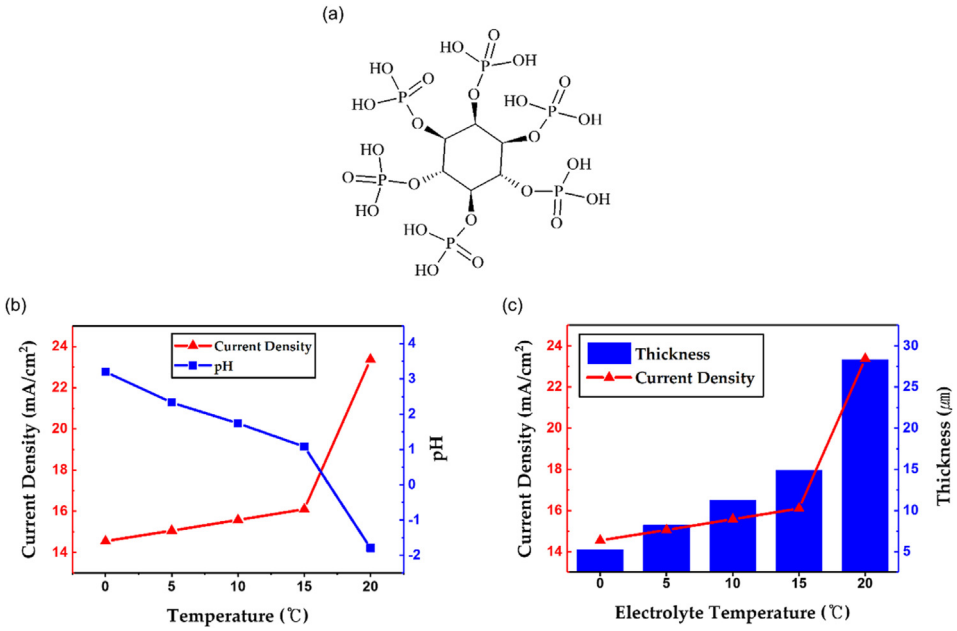

Fig. 2 – (a) Chemical structure of phytic acid, (b) change in the phytic acid bath pH and current density according to electrolyte temperature, and (c) the thickness and growth rate of the AAO films.

film has been grown and pore layer initiation has been completed. Next, the current density rises steadily up to an almost steady. Finally, the current density is constantly kept, and then pore layer growth takes place [32].

Three steps, before the current density stabilizes, take place for a relatively short time, and the current density is constantly kept during the most anodizing process. Therefore, if the current density is measured after sufficient processing time, the current density during most processes can be measured. The current density was measured just before the end of the entire 180 min process time to obtain a representative value for the entire process.

When the temperature of the phytic acid bath rises to 0, 5, 10, 15, 20 °C, the pH decreases to 3.20, 2.23, 1.74, 1.08, −1.79, respectively, but in contrast the current density increases to 14.55, 15.06, 15.58, 16.10 and 23.38 mA/cm^2 (Fig. 2b).

As the temperature increases, H^+ dissociation is activated in the phytic acid, resulting in a change in the pH (Eq. (1)), which is a direct cause of the higher current density. In particular, when the temperature of the phytic acid bath is 20 °C, the current density sharply increases. It is not clear why the current density sharply increases when the anodizing bath temperature is 20 °C. However, the pH also changes rapidly, suggesting that as phytic acid decomposes and some materials are produced that rapidly change the current density and pH results.

As the current density increases, the thickness of the AAO film increases to 5.26, 8.24, 11.26, 14.90, and 28.32 μm (Fig. 2c). The displacement of the AAO film on the aluminum surface is mainly due to the stress caused by electrical deformation, and the growth of the oxide film occurs at the interface between the electrolyte and the aluminum. At this time, it is known that the generated stress is involved in self-organization to form a porous structure [33].

Since AAO film growth stress depends on the anodizing voltage, process temperature, and electrolytes, the structural characteristics of the AAO film, such as pore diameter, are different according to the process conditions. In general, the pore diameter increases with increasing temperature [33]. The change in the pH and current density affects the AAO film growth rate and growing stress. As a result, the growth rate

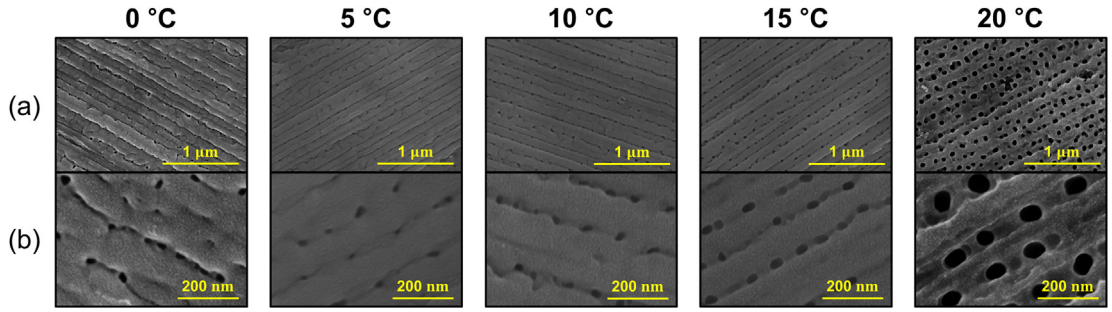

Fig. 3 – FE-SEM image of AAO films surface before Plasma corrosion test: Magnification (a) 50 K, (b) 200 K.

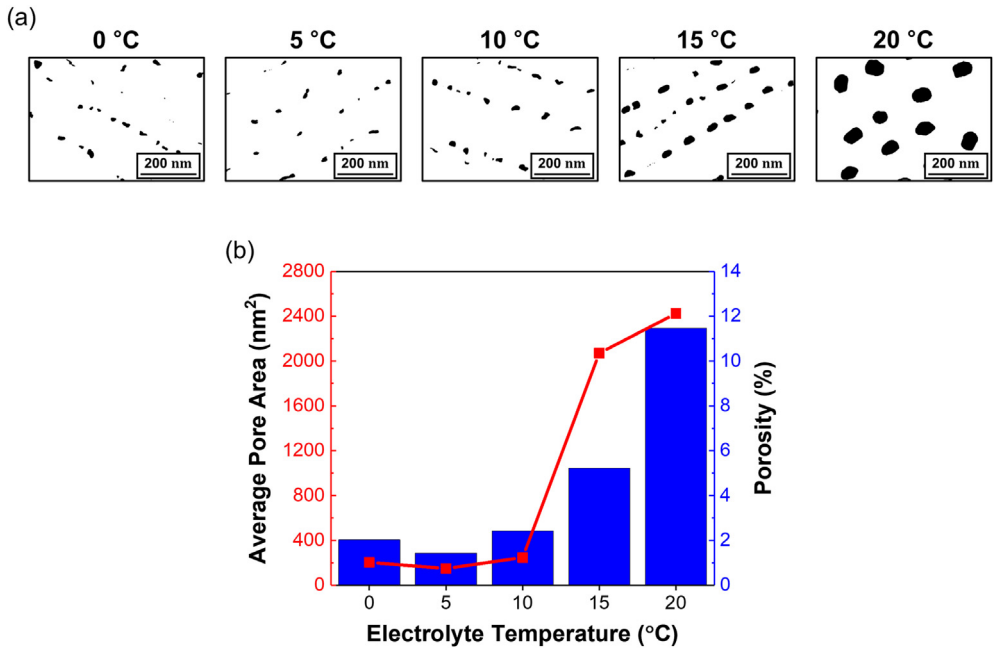

Fig. 4 – (a) AAO film surface pore analysis for SEM images of Fig. 3b using the ImageJ program and (b) its result of average pore area and porosity.

and pore diameter of the AAO film increases at a high temperature (Fig. 3).

Fig. 4a is an analysis of the surface pores of the AAO film before the plasma corrosion test using ImageJ, an image analysis program, and the image of Fig. 3b was used. It can be seen that the area of the pores increases as the temperature of the electrolyte increases, and it shows a tendency to increase rapidly from 15 °C.

Fig. 4b is numerically represented this change in surface morphology. The pore areas were 203 nm^2, 150 nm^2, and 250 nm^2 at 0 °C, 5 °C and 10 °C, respectively. These results are difficult to be seen as a significant difference when considering the non-uniformity of the pores. However, it can be clearly seen that at 15 °C and 20 °C, it increases rapidly to 1830 nm^2 and 2423 nm^2, respectively.

In addition, the porosity was 2.03%, 1.43%, 2.43%, 5.22%, and 11.46% at 0 °C, 5 °C, 10 °C, 15 °C, and 20 °C, respectively, and the same tendency as the pore area appeared. From these results, it can be seen that the increase in the pore area has a dominant effect on the increase in the porosity.

Fig. 5a shows the normalized XRD pattern of the AAO film surface according to the temperature of the phytic acid electrolyte (111) and (222) Aluminum crystal planes are observed by aluminum substrates, and (113) and (104) alpha-alumina crystal planes are observed by AAO films [34–37]. In the case of (111) (222) aluminum crystal plane, and (104) alpha-alumina crystal plane, there was no significant difference depending on the temperature of the phytic acid electrolyte.

However, a distinct difference was observed in the (113) alpha-alumina crystal plane. The relatively high intensity was observed in the AAO films at 0 °C, 5 °C and 10 °C compared to the AAO films with electrolyte temperatures of 15 °C and 20 °C (Fig. 5b). This difference in the intensity of alpha-alumina is an important factor in determining the properties of AAO film, and it has been reported that the more alpha-alumina is formed, the better the properties are [38,39].

On the other hand, the structural characteristics caused by the AAO film growth stress change the electrical and chemical resistance characteristics of the AAO film. Fig. 6a shows the breakdown voltage and breakdown voltage per unit thickness of the AAO film according to the temperature. The breakdown voltage is the threshold voltage that can be borne when the AAO film is used for plasma corrosion protection coatings of equipment parts in the process chamber of semiconductor and display manufacturing. In general, the breakdown voltage strength is known to depend on the thickness [30]. The pores of the AAO film act as air gaps at the electrode - insulation layer interface, so when the same voltage is applied, the larger the pore size, the higher the electrical stress per unit area.

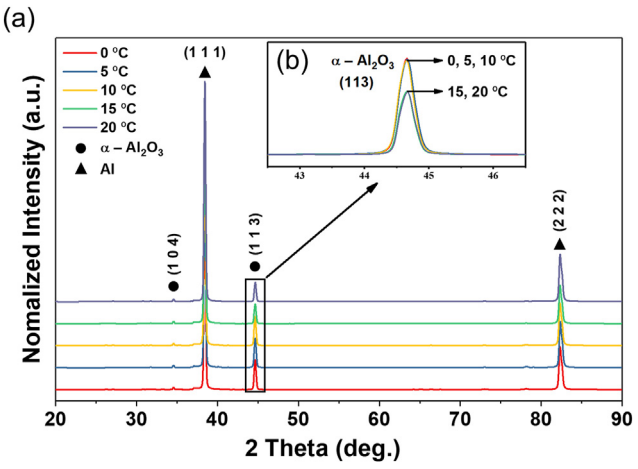

Fig. 5 – Characteristic peak intensity normalized X-ray diffraction patterns of AAO film.

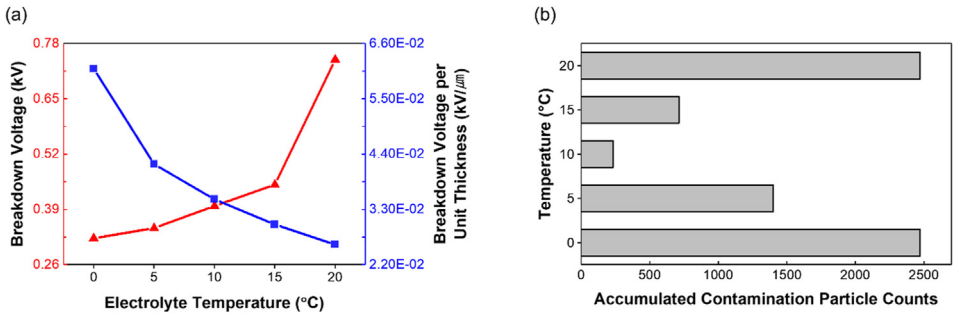

Fig. 6 – (a)The breakdown voltage and breakdown voltage per unit thickness of AAO film and (b) the generation of contamination particles on the AAO film surface by plasma.

Table 3 – After being exposed to the plasma, the AAO films surface component.

Temperature	Element (at. %)			
	Aluminum	Oxygen	Fluorine	Phosphorus
0 °C	26.57	49.47	23.58	0.38
5 °C	22.08	51.35	26.29	0.28
10 °C	24.76	46.16	28.46	0.62
15 °C	21.94	46.21	31.28	0.57
20 °C	22.37	39.06	37.82	0.76

The AAO film grown in the 0 °C phytic acid electrolyte bath has a slow growth rate, so the film is thin, and the breakdown voltage is low. But it has low growing stress, so the pore size is small, and the thin film grows densely, resulting in a high breakdown voltage per unit thickness. In contrast, the growth rate of the AAO film in the 20 °C phytic acid bath is fast with a greater thickness, so the breakdown voltage is high. However, the growth stress is large and the pore size is large, so high electrical stress is applied per unit area, resulting in a lower breakdown voltage per unit thickness.

The change in the thickness and structural characteristics of the AAO film (e.g. example corrosion, crack, etc.) due to the phytic acid bath temperature influences the generation of contamination particles on the AAO film surface by plasma (Fig. 6b) [20,40,41]. The contamination particles by the plasma are generated when Al_2O_3 reacts with fluorine ions, and generates AlF_3, which grows into particles, resulting in the drop-off of the contamination particles at the weakly bonded site [42]. Fig. 5 and Table 3 show the FE-SEM image and EDS analysis results of the AAO film surface, respectively, after exposure to plasma with etching gas (Table 2). After the AAO films are exposed to the plasma, the surface cracks due to thermal stress and physicochemical etching by CF_4 and Ar gas. This leads to a component change in the AAO film surface.

In the AAO film grown in 0 °C phytic acid bath, contamination particles can be seen to be easily dropped due to surface cracks caused by thermal stress, and many contamination particles are generated [20,40,41]. However, the AAO films grown in 15 °C and 20 °C phytic acid baths increased the number of contamination particles, despite little surface cracking. This is thought to be due to two factors.

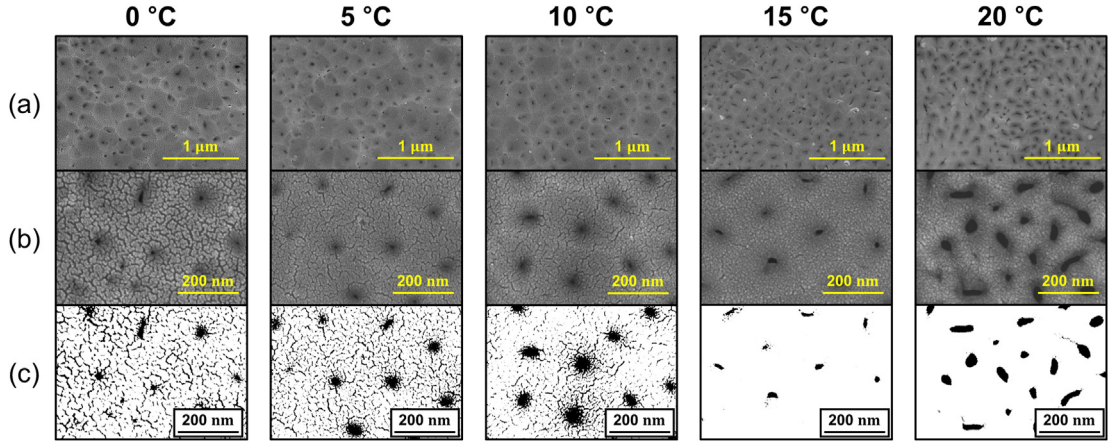

Fig. 7 – FE-SEM images of the AAO films surface morphology of after plasma corrosion test (Magnification (a) 50 K, (b) 200 K) and (c) the surface analysis of crack using ImageJ program.

First, the surface area is widened due to the large pore size, and the reaction rate with the plasma increases, thereby causing the contamination particles to grow by reacting with the fluorine ion at a relatively high rate (Table 3 and Fig. 7a, b). Next, due to the fast growth rate of the AAO film, its orientation is poor and the density is relatively low, resulting in the easy drop-off of contamination particles at a weak bonding force between the atoms.

Typically, the surface temperature of the Al_2O_3 film exposed to plasma increases, so the temperature of the AAO film was raised to about 400 K for 10 min with the plasma that was used for the plasma corrosion test in this study. Then, it was maintained at a constant temperature during the plasma corrosion test. At this time, the AAO film is stressed due to the difference in the thermal expansion coefficient between the Al substrate and the AAO film, and its thermal stress causes cracking in the AAO film surface (Fig. 7). The AAO film grown in 0 °C phytic acid bath is easily cracked because of its thinness, despite the lower growth stress. The surface cracks of the AAO film gradually decrease with a thicker AAO film, and almost no cracking is seen in the AAO film grown in the phytic acid bath above 15 °C.

On the other hand, the grain boundaries of the AAO film that is generated through physicochemical etching by CF_4 and Ar gas when grown in 0 °C phytic acid bath can be confirmed. However, as the temperature of the phytic acid bath increases, grain boundaries are not observed. The grain boundaries of the AAO film are affected by the Al substrate [30]. The boundaries of the AAO film are expected to be oriented along the Al substrate in the low-temperature phytic acid bath because of the slow growth rate of AAO films, but they are not oriented in the high-temperature phytic acid bath because of the rapid growth rate of the AAO films.

4. Conclusions

This study investigated the changes in the AAO film characteristics according to the temperature of the phytic acid electrolytes, and its applicability was confirmed as a coating material for plasma corrosion protection of equipment parts in the process chamber for semiconductor and display manufacturing. The temperature of the phytic acid bath affects the current density by changing the pH of the electrolytes. As a result, the pore size, density, and orientation of the AAO film change depending on the temperature of the phytic acid bath. The characteristics as a coating for plasma corrosion protection changed due to the structural characteristics of the AAO film grown in the phytic acid bath. The AAO films grown in high-temperature phytic acid baths have a low density due to their high growth rate, and this caused a lower breakdown voltage per unit area. In addition, relatively many contamination particles are generated when exposed to plasma. However, the AAO films grown in low-temperature phytic acid baths have low productivity due to low growth rates, and cracks are easily generated by thermal stress.

Consequently, to obtain an AAO film having high corrosion resistance by plasma and a small number of pollutant particles, a method of maintaining a high thickness in a low-temperature phytic acid electrolyte bath may be proposed. In the case of the anodizing process conducted in this paper, the thickness of the AAO film was different, respectively, because the time was constant regardless of the temperature of the phytic acid electrolyte bath. Therefore, if the AAO film is grown thick in a 10 °C phytic acid electrolyte bath, it is expected that the best coating film to prevent plasma corrosion can be grown.

Declaration of Competing Interest

The authors declare that they have no known competing financial interests or personal relationships that could have appeared to influence the work reported in this paper.

Acknowledgment

This research was supported by the Material parts technology development program of the Ministry of Trade, Industry and Energy Grant of South Korea (20003660) and the Characterization platform for advanced materials funded by Korea Research Institute of Standards and Science (KRISS–2021–GP2021–0011–10).

REFERENCES

[1] Shih H-H, Tzou S-L. Study of anodic oxidation of aluminum in mixed acid using a pulsed current. Surf Coating Technol 2000;124:278–85.
[2] Osman MM. Corrosion inhibition of aluminium-brass in 3.5% NaCl solution and sea water. Mater Chem Phys 2001;71:12–6.
[3] Hao Q, Huang H, Fan X, Hou X, Yin Y, Li W, et al. Facile design of ultra-thin anodic aluminum oxide membranes for the fabrication of plasmonic nanoarrays. Nanotechnology 2017;28.
[4] Sharma K, Islam SS. Optimization of porous anodic alumina nanostructure for ultra high sensitive humidity sensor. Sensor Actuator B Chem 2016;237:443–51.
[5] Mozalev A, Bendova M, Vazquez RM, Pytlicek Z, Llobet E, Hubalek J. Formation and gas-sensing properties of a porous-alumina-assisted 3-D niobium-oxide nanofilm. Sensor Actuator B Chem 2016;229:587–98.
[6] Kikuchi T, Kunimoto K, Ikeda H, Nakajima D, Suzuki RO, Natsui S. Fabrication of anodic porous alumina via galvanostatic anodizing in alkaline sodium tetraborate solution and their morphology. J Electroanal Chem 2019;846:113152.
[7] Lee SS, Kim MJ, Chung CW, Song JB, Oh SG, Kim JT, et al. Degradation test for an anodic aluminum oxide film in plasma etching. J Kor Phys Soc 2019;74:1046–51.
[8] Shin J, Kim M, Song J, Jeong N, Kim J, Yun J. Fluorine Plasma Corrosion Resistance of Anodic Oxide Film Depending on Electrolyte Temperature 2018;27:9–13.
[9] Garcia-Vergara SJ, Skeldon P, Thompson GE, Habazaki H. A tracer investigation of chromic acid anodizing of aluminium. Surf Interface Anal 2007;39:860–4.

[10] Vrublevsky I, Parkoun V, Schreckenbach J, Marx G. Study of porous oxide film growth on aluminum in oxalic acid using a re-anodizing technique. Appl Surf Sci 2004;227:282–92.
[11] Surganov VF, Gorokh GG. Anodic oxide cellular structure formation on aluminum films in tartaric acid electrolyte. Mater Lett 1993;17:121–4.
[12] Stojadinovic S, Vasilic R, Nedic Z, Kasalica B, Belca I, Zekovic L. Photoluminescent properties of barrier anodic oxide films on aluminum. Thin Solid Films 2011;519:3516–21.
[13] Li YD, Zhang Y, Li SM, Zhao PZ. Influence of adipic acid on anodic film formation and corrosion resistance of 2024 aluminum alloy. Trans Nonferrous Met Soc China 2016;26:492–500 (English Ed.
[14] Suzuki Y, Kawahara K, Kikuchi T, Suzuki RO, Natsui S. Corrosion-resistant porous alumina formed via anodizing aluminum in etidronic acid and its pore-sealing behavior in boilingwater. J Electrochem Soc 2019;166:C261–9.
[15] Choudhary RK, Mishra P, Kain V, Singh K, Kumar S, Chakravartty JK. Scratch behavior of aluminum anodized in oxalic acid: effect of anodizing potential. Surf Coating Technol 2015;283:135–47.
[16] Kikuchi T, Nishinaga O, Natsui S, Suzuki RO. Self-ordering behavior of anodic porous alumina via selenic acid anodizing. Electrochim Acta 2014;137:728–35.
[17] Akiya S, Kikuchi T, Natsui S, Sakaguchi N, Suzuki RO. Self-ordered porous alumina fabricated via phosphonic acid anodizing. Electrochim Acta 2016;190:471–9.
[18] Knörnschild G, Poznyak AA, Karoza AG, Mozalev A. Effect of the anodization conditions on the growth and volume expansion of porous alumina films in malonic acid electrolyte. Surf Coating Technol 2015;275:17–25.
[19] Kikuchi T, Nishinaga O, Natsui S, Suzuki RO. Fabrication of anodic nanoporous alumina via acetylenedicarboxylic acid anodizing. ECS Electrochem. Lett. 2014;3:25–8.
[20] Song J-B, Kim J-T, Oh S-G, Shin J-S, Chun J-R, Yun J-Y. Effect of sealing time of anodic aluminum oxide (AAO) film for preventing plasma damage. Sci Adv Mater 2015;7:127–32.
[21] Gupta RK, Mensah-Darkwa K, Sankar J, Kumar D. Enhanced corrosion resistance of phytic acid coated magnesium by stearic acid treatment. Trans Nonferrous Met Soc China 2013. English Ed.
[22] Zhang RF, Zhang SF, Duo SW. Influence of phytic acid concentration on coating properties obtained by MAO treatment on magnesium alloys. Appl Surf Sci 2009;255:7893–7.
[23] Shi H, Han EH, Liu F, Kallip S. Protection of 2024-T3 aluminium alloy by corrosion resistant phytic acid conversion coating. Appl Surf Sci 2013;280:325–31.
[24] Wang S, Peng H, Shao Z, Zhao Q, Du N. Sealing of anodized aluminum with phytic acid solution. Surf Coating Technol 2016;286:155–64.
[25] Pan F, Yang X, Zhang D. Chemical nature of phytic acid conversion coating on AZ61 magnesium alloy. Appl Surf Sci 2009;255:8363–71.
[26] Guo X, Du K, Guo Q, Wang Y, Wang R, Wang F. Effect of phytic acid on the corrosion inhibition of composite film coated on Mg-Gd-Y alloy. Corrosion Sci 2013;76:129–41.
[27] Yang X, Li L, He J, Guo H, Zhang J. In vitro corrosion and bioactivity study of surface phytic acid modified AZ31 magnesium alloy. Mater Sci Appl 2014;5:59–65.
[28] Zhang M, Cai S, Shen S, Xu G, Li Y, Ling R, et al. In-situ defect repairing in hydroxyapatite/phytic acid hybrid coatings on AZ31 magnesium alloy by hydrothermal treatment. J Alloys Compd 2016;658:649–56.
[29] Crea F, De Stefano C, Milea D, Sammartano S. Formation and stability of phytate complexes in solution. Coord Chem Rev 2008;252:1108–20.
[30] Song JB, Choi E, Oh SG, So J, Lee SS, Kim JT, et al. Improved reliability of breakdown voltage measurement of yttrium oxide coatings by plasma spray. Ceram Int 2019;45:22169–74.
[31] Chen QC, Li BW. Separation of phytic acid and other related inositol phosphates by high-performance ion chromatography and its applications. J Chromatogr, A 2003;1018:41–52.
[32] Theohari S, Kontogeorgou C. Effect of temperature on the anodizing process of aluminum alloy AA 5052. Appl Surf Sci 2013;284:611–8.
[33] Aerts T, Dimogerontakis T, De Graeve I, Fransaer J, Terryn H. Influence of the anodizing temperature on the porosity and the mechanical properties of the porous anodic oxide film. Surf Coating Technol 2007;201:7310–7.
[34] Li SY, Xiang XG, Ma BH, Meng XD. Facile preparation of diverse alumina surface structures by anodization and superhydrophobic surfaces with tunable water droplet adhesion. J Alloys Compd 2019;779:219–28.
[35] Li J, Zhao S, Du F, Zhou Y, Yu H. One-step fabrication of superhydrophobic surfaces with different adhesion via laser processing. J Alloys Compd 2018;739:489–98.
[36] Zhang Y, Yu X, Wu H, Wu J. Facile fabrication of superhydrophobic nanostructures on aluminum foils with controlled-condensation and delayed-icing effects. Appl Surf Sci 2012;258:8253–7.
[37] Masuda T, Asoh H, Haraguchi S, Ono S. Fabrication and characterization of single phase α-alumina membranes with tunable pore diameters. Materials 2015;8:1350–68.
[38] Xiangfeng M, Guoying W, Hongliang G, Yundan Y, Ying C, Dettinger H. Anodization for 2024 al alloy from sulfuric-citric acid and anticorrosion performance of anodization films. Int. J. Electrochem. Sci. 2013;8:10660–71.
[39] Boldrini DE, Yañez MJ, Tonetto GM. Influence of the anodizing process variables on the acidic properties of anodic alumina films. Braz J Chem Eng 2017;34:1043–53.
[40] Liu W, Zuo Y, Chen S, Zhao X, Zhao J. The effects of sealing on cracking tendency of anodic films on 2024 aluminum alloy after heating up to 300 °C. Surf Coating Technol 2009;203:1244–51.
[41] Zhao X, Liu W, Zuo Y, Yang L. The cracking behaviors of anodic films on 1050 and 2024 aluminum alloys after heating up to 300 °C. J Alloys Compd 2009;479:473–9.
[42] Cao YC, Zhao L, Luo J, Wang K, Zhang BP, Yokota H, et al. Plasma etching behavior of Y 2 O 3 ceramics: comparative study with Al 2 O 3. Appl Surf Sci 2016;366:304–9.